

07

## Direct current modulation of high power semiconductor lasers by high-frequency limit-cycle oscillations in gallium arsenide avalanche diodes

© A.V. Rozhkov, P.B. Rodin

Ioffe Institute, St. Petersburg, Russia  
E-mail: rozh@hv.ioffe.rssi.ru

Received July 2, 2025

Revised September 1, 2025

Accepted September 1, 2025

High-frequency limit-cycle oscillations generated by reversely biased high-voltage diode operated in simplistic electrical circuit are applied for the direct current modulation of power semiconductor laser. Oscillation frequency is 2–2.4 GHz. The avalanche diode is connected by means of a strip line in-series with heterolaser equipped by tunnel-connected emitters and  $50\ \Omega$  load. It has been observed that oscillations of the laser current and oscillations of the photodetector signal have the same frequency. The peak power of optical signal  $P_m$  at the maximum laser current  $\sim 2.0\ \text{A}$  was  $P_m \sim 5.5\ \text{W}$  for the half-width duration of the optical pulse  $\sim 180\ \text{ps}$ .

**Keywords:** direct current modulations, impact-ionization instabilities, avalanche diodes.

DOI: 10.61011/TPL.2026.01.62815.20424

The formation of short high power laser pulses with a high repetition frequency is a pressing scientific and technical challenge [1–16]. Direct current modulation of lasers [2] with nano- or subnanosecond current pulses is one potential solution to this problem. Unlike phase locking and Q-modulation methods [3–7], direct current modulation with short pulses [8–12] allows one to use commercially available lasers instead of specially designed laser structures. However, this method imposes strict requirements on a semiconductor driver that generates short current pulses with a high repetition frequency [10–12]. In the present study, we demonstrate experimentally the feasibility of direct high-frequency modulation of laser radiation using a new physical phenomenon in avalanche diodes: high-frequency limit-cycle oscillations of current in the gigahertz frequency range [17]. Deeply modulated laser radiation at 2.4 GHz frequency achieved in experiments with a commercially available laser and avalanche diode operating in the mentioned above regime used as a driver. The FWHM of a single pulse was  $t_{\text{FWHM}} = 180\ \text{ps}$ , and the duration of a train of periodic pulses of quasi-harmonic shape with repetition frequency  $f_{\text{PRF}} = 2.4\ \text{GHz}$  varied from 20 to 200 ns.

Limit-cycle oscillations of current in the diode used as a high-frequency driver emerge spontaneously due to a soft oscillatory instability of the steady state on the reverse „avalanche“ branch of the current–voltage curve (CVC) and correspond to the nonlinear avalanche-transit regime [17]. Limit-cycle oscillations in high-power silicon diodes have a similar physical mechanism [18]. Unlike the case of classical Impact Avalanche Transit Time (IMPATT) diodes [19], limit-cycle oscillations [17,18] proceed in a simplistic electrical circuit without a resonator, which includes only the diode and an in-series ohmic load.

GaAs  $p^+ - p - i - n - n^+$  diodes with an oscillation frequency of 2–2.4 GHz, diameter  $d = 500\ \mu\text{m}$ , and breakdown voltage  $U_b \approx 380\ \text{V}$  were used in experiments. They have been described in detail in recent paper [20] and fabricated by Rozhkov et al. in the early 2000s [21]. The diode was connected in series with a commercially available SPLPL90\_3 laser with three tunnel-coupled emitters (emission maximum at a wavelength of 905 nm; aperture,  $200 \times 10\ \mu\text{m}$ ) and a  $50\ \Omega$  load using a coplanar microwave strip line (Fig. 1). A quasi-rectangular reverse-polarity pulse with amplitude  $U_1$ , duration of 20–200 ns, repetition frequency of 1–10 kHz and constant reverse bias  $U_2$  was applied to the input of the line. The experimental setup allowed us to vary the values of  $U_1$  and  $U_2$ . According to [17], condition  $U_1 + U_2 > U_b$  must be satisfied in order to observe self-excitation of oscillations in the diode. With two different trigger generators, the leading-edge time of the pulse  $U_1$  was 200 ps or 10 ns. Impedance matching of the  $50\ \Omega$  coaxial strip line, which includes the high-voltage GaAs diode and the laser, and the measuring channel suppresses the reflection of a laser pulse though some reduction of the modulated current amplitude.

A GaAs photodiode fabricated by liquid-phase epitaxy (diameter,  $150\ \mu\text{m}$ ; photosensitive area  $\sim 5 \cdot 10^{-5}\ \text{cm}^2$ ) was used as a laser radiation detector. Detection was performed under reverse bias  $U_3 = 60\ \text{V}$ . A focusing lens system was mounted between the laser and the photodiode. Load voltage  $U_R(t)$  in the laser supply circuit (channel 1) and voltage  $U_{ph}(t)$  in the detecting photodiode circuit (channel 2) were recorded by Tektronix DPO 70404C digital dual-channel oscilloscope with frequency band of 4 GHz (Fig. 1). A set of broadband attenuators was used to measure voltage  $U_R(t)$  (channel 1). The oscilloscope records in channels 1 and

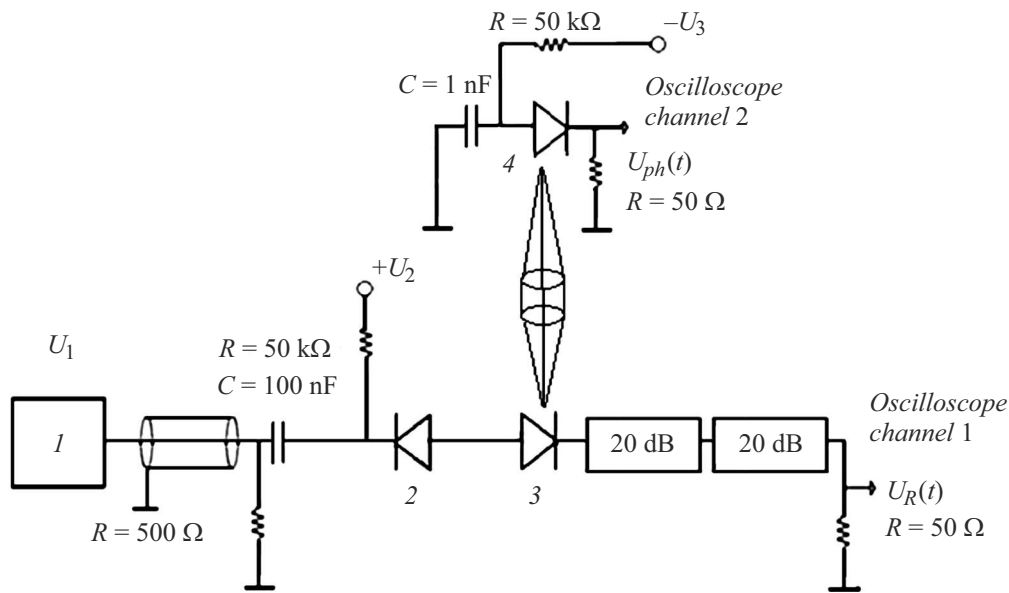


**Figure 1.** Sketch of the experimental setup. 1 — Pulse voltage generator, 2 — high-voltage GaAs avalanche diode, 3 — SPLPL90\_3 laser diode, and 4 — photodiode based on an epitaxial GaAs  $p$ - $i$ - $n$  structure.

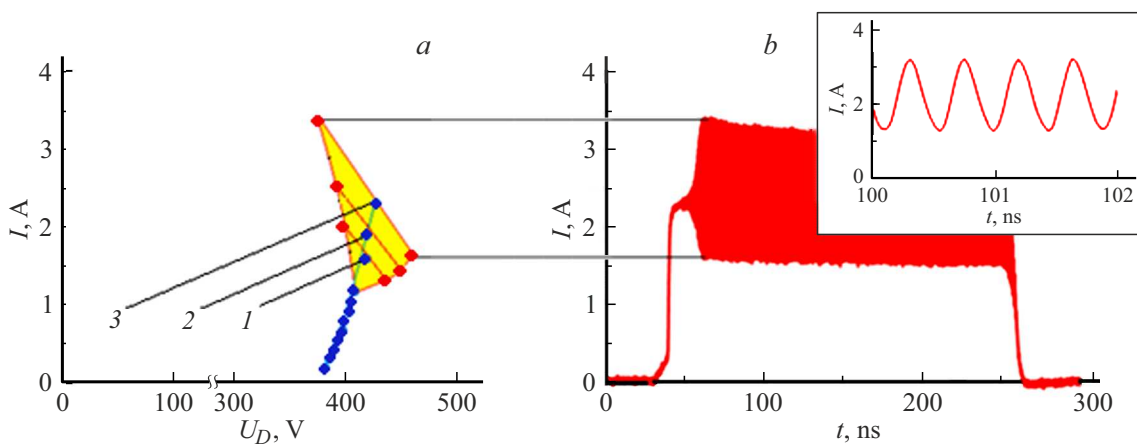


**Figure 2.** Experimental CVC with „phase trajectories“ ( $I$ ,  $U_D$ ) (1–3) (a) and time dependence  $I(t)$  (b) for a „soft“ transition to high-frequency oscillations under a slow (within 10 ns) rise of GaAs diode voltage  $U_1$ . In the experiment, the amplitude of pulses  $U_1$  and voltage  $U_2$  (in V) for the phase trajectories indicated in panel a were as follows: 1 — 320, 165; 2 — 320, 175; 3 — 320, 225. The inset in panel b presents a detailed view of oscillations. A color version of the figure is provided in the online version of the paper.

2 determined the time dependence of current through the laser  $I(t) = U_R(t)/R$  and the photodiode  $i(t) = \Delta U_{ph}(t)/R$ .

Figure 2 presents the results of experimental measurements of high-frequency current oscillations  $I(t)$  (channel 1) and their dependence on the amplitude of applied pulse  $U_1$  and initial bias  $U_2$ . These oscillations are shown in Fig. 2, a on the diode current–voltage plane ( $I$ ,  $U_D$ ) together with the reverse CVC of the diode. When the avalanche current is below 1 A, steady states on the reverse CVC branch are stable (blue dots in Fig. 2, a). When the current exceeds this value, limit-cycle oscillations emerge spontaneously. Red segments (curves 1–3 in Fig. 2, a), the slope of which is set by the load curve, correspond to limit-cycle oscillations on

the plane ( $I$ ,  $U_D$ ). Limit-cycle oscillations arise as a result of „soft“ instability of the steady state. The instability is illustrated in Fig. 2, b through the example of oscillations corresponding to phase trajectory 3 (Fig. 2, a). This trajectory emerges from an unstable steady state with a current of 2.5 A, which corresponds to the intersection of the unstable part of the reverse CVC branch and the load curve. For brevity, we call this state the „working point.“ Working points with operating currents of 1.5 and 2 A correspond to trajectories 1 and 2 in Fig. 2, a, respectively. The current through the diode and the laser was set by the amplitude of trigger pulse  $U_1$  and initial reverse bias  $U_2$  of the diode. It follows from Fig. 2, a that the amplitude of oscillations and,

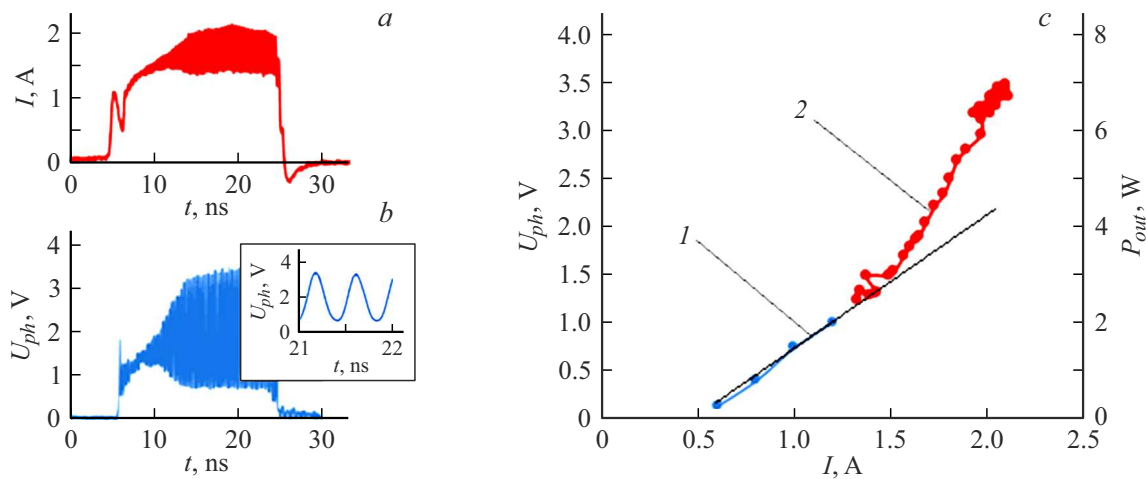


**Figure 3.** Oscilloscope records of the laser modulation current (a) and the photoresponse of the GaAs  $p-i-n$  photodiode (b) for a quasi-stationary current of 2.0 A. Amplitude and watt–ampere calibration (1) and output high-frequency (2) dependences for the current modulation regime of the TO-packaged SPLPL90\_3 laser (c). The inset in panel b presents a detailed view of photoresponse oscillations.

accordingly, the depth of laser current modulation increase with increasing reverse voltage. When voltages  $U_1$  and  $U_2$  increased further, irreversible degradation of the diode was observed in several cases.

Figures 3, a, b show the oscilloscope records of laser modulation current  $I(t)$  and response  $U_{ph}(t) = Ri(t)$  of the detecting photodiode for a pulse duration of 20 ns. Deep high-frequency modulation of laser radiation was achieved. Measurements were carried out within the range of  $U_1$  and  $U_2$  values corresponding to the variation of stationary (unstable) avalanche current through the laser from 1 to 2.5 A. Modulation frequency  $f_{PRF}$  and FWHM signal duration  $t_{FWHM}$  in these regimes were 2.4 GHz and 180 ps, respectively. Note that the minimum signal duration  $t_{FWHM}$  specified by the manufacturer of the used SPLPL90\_3 laser is 1 ns.

With the positions of the laser, focusing lenses, and the photodetector fixed, amplitude and watt–ampere dependences were determined for the pulsed (calibration dependence 1) and periodic (output high-frequency dependence 2) current pumping regimes (Fig. 3, c). The relative values of photoresponse signals and the rated watt–ampere characteristic of the SPLPL90\_3 laser were used to estimate the absolute values of pulse power. Peak optical signal power  $P_{peak}$  was  $\sim 5.5$  W at a laser current of  $\sim 2.0$  A. The radiation power increased noticeably under high-frequency current pumping. This phenomenon may be associated with the well-known resonant increase in intensity of laser radiation at a current pumping frequency close to the frequency of relaxation oscillations in the laser [22].

To conclude, let us discuss the obtained results in the overall context of research on the formation of short laser pulses with a high repetition frequency for communication systems, lidars, and radio photonics [2–16]. Physical methods for generation of short pulses include mode locking, Q-modulation [3–7], and direct current modulation

with short (nanosecond) current pulses (often in the gain-switching regime) [8–12]. The first two methods provide an opportunity to obtain record-short pulses (down to  $t_{FWHM} \sim 1$  ps) with high repetition frequency  $f_{PRF}$  (up to 100 GHz) in specially designed laser structures. However, the energy of such pulses is relatively low ( $E \leq 0.1$  nJ) [3–7]. The key role in direct current modulation is played by the pulse semiconductor driver [8–12].

Silicon bipolar transistors [8,10], GaN HEMTs (high-electron-mobility transistors) [11], and GaAs S-diodes [12] were investigated as drivers. GaAs/AlGaAs thyristor lasers [13–15], which combine a driver and an optical emitter in a single crystal, were also developed. The main parameters of pulses taken from studies into direct current modulation [10–15] are listed in the table. The table also presents the results reported in [16], where direct current modulation with a short pulse and Q-modulation were combined. The efficiency is estimated using parameter  $M_{eff} \equiv f_{PRF} P_{peak} t_{FWHM}$ , which characterizes the average power of the modulated optical signal. It can be seen from the table that pulse energy  $E \sim 10$ –100 nJ was obtained at a pulse duration of 0.1–2 ns [10–16]. This power is sufficient for use in lidars [16], and shorter pulse durations  $t_{FWHM}$  are actually not required in practice, since the speed performance of  $p-i-n$ -diodes (radiation detectors) is limited. The repetition frequency is limited at the level of  $\sim 100$  kHz for all listed drivers [8,10,12–16] except GaN HEMTs [9,11], which reach a repetition frequency of 100 MHz. It is for GaN HEMTs that the highest value of modulation efficiency parameter  $M_{eff} \sim 1$  W was achieved. Increasing the repetition frequency is a substantial challenge for all known types of direct current modulation drivers [8,10,16] and thyristor lasers [13–15]. All methods are characterized by a high pulse period-to-duration ratio:  $t_{FWHM} \ll (f_{PRF})^{-1}$ .

Comparison of the main parameters of laser pulses corresponding to different semiconductor drivers used for direct current modulation

Pulse generator type	$P_{peak}$ , W	$t_{FWHM}$ , ns	$f_{PRF}$ , GHz	$E$ , nJ	$M_{eff}$ , W
Si bipolar transistors [10]	43–180	0.8–1.9	$(1-2) \cdot 10^{-4}$	82–144	$(0.8-3) \cdot 10^{-2}$
GaN HEMTs [11]	30	0.5	0.1	15	$\sim 1$
GaAs S-diode [12]	60	1.5	$10^{-4}$	90	$9 \cdot 10^{-3}$
GaAs/AlGaAs thyristor laser [13]	6	0.95	$1.3 \cdot 10^{-4}$	5.7	$7.4 \cdot 10^{-4}$
GaAs/AlGaAs thyristor laser [14]	22	0.11	$10^{-4}$	2.42	$2.4 \cdot 10^{-4}$
GaAs/AlGaAs thyristor laser [15]	39.5	0.12	$10^{-4}$	4.74	$1.1 \cdot 10^{-3}$
„Gain-switching“ laser with saturable absorber [16]	35	0.08	$10^{-4}$	2.8	$3.2 \cdot 10^{-3}$
GaAs avalanche diode (present study)	5.5*	0.18*	2.4*	$\sim 1$	2.4*

\*For a train of quasi-harmonic pulses with a duration  $\leq 200$  ns.

In contrast, high-frequency modulation implemented here corresponds to the limit case of a low pulse period-to-duration ratio:  $t_{FWHM} \approx (f_{PRF})^{-1}$ . Peak pulse power  $P_{peak} = 5.5$  W and pulse energy  $E = 1$  nJ are somewhat lower, but comparable to the results reported in [8–16]. Pulse FWHM  $t_{FWHM} \approx 0.18$  ns falls within the same sub-nanosecond range, but pulse repetition frequency  $f_{PRF}$  is several orders of magnitude higher. Owing to this, the modulation efficiency parameter reaches the level of  $M_{eff} = 2.4$  W. However, it is not entirely correct to compare directly the periodic optical signal of a quasi-harmonic shape produced here (Fig. 3) with pulsed periodic signals with a high period-to-duration ratio obtained in [10–16] with the use of pulsed rather than frequency drivers.

Combined with a detector tuned to a gigahertz „carrier“ frequency, nanosecond trains of quasi-harmonic pulses obtained by the method proposed above may be used for laser ranging and detection and to implement amplitude, phase, and frequency modulation in combined radio-over-fiber communication lines. The uniformity of limit-cycle oscillations over the diode cross-section [17] potentially allows one to reduce the series load and expand the range of current modulation by increasing the diode area. It is also possible to use higher-frequency avalanche diodes [17]. Note also that, just like S-diodes [12], a diode operating in the regime of self-excitation of avalanche limit-cycle oscillations allows for low-inductive assembly with a semiconductor laser, potentially removing the need for a strip line in practical applications.

Thus, the feasibility of current modulation of a semiconductor laser at a frequency of 2.4 GHz by an avalanche GaAs diode, which operates in the regime of self-excitation of limit-cycle oscillations, in a simplistic circuit with a series connection of the laser and the diode was demonstrated. The obtained results are of potential interest for radio photonics.

## Acknowledgments

The authors wish to thank G.S. Sokolovskii for fruitful discussions and helpful advice.

## Conflict of interest

The authors declare that they have no conflict of interest.

## References

- [1] E.U. Rafailov, E. Avrutin, in *Semiconductor lasers*, ed. by A. Baranov, E. Tournie (Woodhead Publ., Oxford, 2013), p. 149. DOI: 10.1533/9780857096401.1.149
- [2] N.H. Zhu, Z. Shi, Z.K. Zhang, Y.M. Zhen, C.W. Zou, Z.P. Zhao, Y. Liu, W. Li, M. Li, *IEEE J. Select. Top. Quantum Electron.*, **24** (1), 1500219 (2018). DOI: 10.1109/JSTQE.2017.2720959
- [3] A.G. Deryagin, D.V. Kuxsenkov, V.I. Kuchinskii, E.L. Portnoi, I.Yu. Khrushchev, *Electron. Lett.*, **30** (4), 309 (1994). DOI: 10.1049/el:19940238
- [4] X. Li, H. Wang, Z. Qiao, X. Guo, W. Wang, G.I. Ng, Yu. Zhang, Y. Xu, Z. Niu, C. Tong, C. Liu, *Opt. Express*, **26** (7), 8289 (2018). DOI: 10.1364/OE.26.008289
- [5] R. Morita, T. Inoue, M.De Zoysa, K. Ishizaki, S. Noda, *Nat. Photon.*, **15**, 311 (2021). DOI: 10.1038/s41566-021-00771-5
- [6] H. Wang, L. Kong, A. Forrest, D. Bajek, S.E. Hagggett, X. Wang, B. Cui, J. Pan, Y. Ding, M.A. Catalung, *Opt. Express*, **21** (22), 25940 (2014). DOI: 10.1364/OE.22.025940
- [7] I.M. Gadzhiyev, M.S. Buyalo, A.S. Payusov, A.E. Gubenko, S.S. Mikhrin, V.N. Nevedomsky, E.L. Portnoi, *Tech. Phys. Lett.*, **44** (11), 965 (2018). DOI: 10.1134/S1063785018110068.
- [8] M. Hintikka, J. Kostamovaara, *IEEE Sens. J.*, **18** (3), 1047 (2018). DOI: 10.1109/JSEN.2017.2777501
- [9] V.M. Andreev, D.F. Zaitsev, N.Yu. Novikov, V.S. Kalinovskii, D.V. Mordasov, S.O. Slipchenko, I.S. Tarasov, A.I. Fadeev, *Radiotekhnika*, **80** (11), 177 (2016) (in Russian).
- [10] S. Vainshtein, V. Zemlyakov, V. Egorin, A. Maslvtsov, A. Filimonov, *IEEE Trans. Power Electron.*, **34** (4), 3689 (2019). DOI: 10.1109/TPEL.2018.2853563
- [11] A. Liero, A. Klehr, S. Schwertfeger, T. Hoffmann, W. Heinrich, in *2010 Proc. IEEE MTT-S Int. Microwave Symp.* (Anaheim, CA, 2010), p. 1110. DOI: 10.1109/MWSYM.2010.5517952
- [12] S. Vainshtein, I. Prudaev, G. Duan, T. Rahkonen, *Solid State Commun.*, **365** (7), 115111 (2023). DOI: 10.1016/j.ssc.2023.115111

- [13] S.O. Slipchenko, A.A. Podoskin, V.S. Golovin, D.N. Romanovich, V.V. Shamakhov, D.N. Nikolaev, I.S. Shashkin, N.A. Pikhtin, T.A. Bagaev, M.A. Ladugin, A.A. Marmalyuk, V.A. Simakov, *Opt., Express*, **27** (22), 31446 (2019).  
DOI: 10.1364/OE.27.031446
- [14] A.A. Podoskin, I.V. Shushkanov, V.V. Shamakhov, A.E. Rizaev, M.I. Kondratov, A.A. Klimov, S.V. Zazulin, S.O. Slipchenko, N.A. Pikhtin, *Bull. Lebedev Phys. Inst.*, **50** (Suppl. 5), S513 (2023).  
DOI: 10.3103/S1068335623170104.
- [15] S. Slipchenko, A. Podoskin, I. Shushkanov, A. Rizaev, M. Kondratov, V. Shamakhov, V. Kapitonov, K. Bakhvalov, A. Grishin, T. Bagaev, M.A. Ladugin, A. Marmalyuk, V. Simakov, N. Pikhtin, *Photonics*, **12**, 130 (2025).  
DOI: 10.3390/photonics12020130
- [16] B. Ryvkin, E. Avrutin, J. Kostamovaara, *J. Semicond. Sci. Technol.*, **32**, 025015 (2017).  
DOI: 10.1088/1361-6641/32/2/025015
- [17] A.V. Rozhkov, M.S. Ivanov, P.B. Rodin, *Tech. Phys. Lett.*, **50** (10), 91 (2024).  
DOI: 10.61011/TPL.2024.10.60124.19977.
- [18] S.K. Lyubutin, S.N. Rukin, B.G. Slovikovsky, S.N. Tsyranov, *Semiconductors*, **47** (5), 670 (2013).  
DOI: 10.1134/S1063782613050151.
- [19] A.S. Tager, *Sov. Phys. Usp.*, **9** (6), 892 (1967).  
DOI: 10.1070/PU1967v009n06ABEH003231.
- [20] A.V. Rozhkov, M.S. Ivanov, P.B. Rodin, *Tech. Phys. Lett.*, **48** (8), 61 (2022). DOI: 10.21883/TPL.2022.08.55065.19271.
- [21] V.I. Korol'kov, A.V. Rozhkov, L.A. Petropavlovskaya, *Tech. Phys. Lett.*, **27** (9), 731 (2001). DOI: 10.1134/1.1405242.
- [22] A.E. Zhukov, M.V. Maksimov, *Sovremennye inzhetsionnye lazery* (Izd. Politekh. Univ., SPb., 2009) (in Russian).

*Translated by D.Safin*